

This article was downloaded by:

On: 26 January 2011

Access details: *Access Details: Free Access*

Publisher *Taylor & Francis*

Informa Ltd Registered in England and Wales Registered Number: 1072954 Registered office: Mortimer House, 37-41 Mortimer Street, London W1T 3JH, UK



## Liquid Crystals

Publication details, including instructions for authors and subscription information:

<http://www.informaworld.com/smpp/title~content=t713926090>

### Thermotropic liquid-crystalline systems containing methylated rings

G. Costa<sup>a</sup>; A. Minicucci<sup>b</sup>; V. Trefiletti<sup>a</sup>; B. Valenti<sup>b</sup>

<sup>a</sup> Centro di Studi Chimico-Fisici di Macromolecole Sintetiche e Naturali, CNR, Genova, ITALY <sup>b</sup>

Istituto di Chimica Industrial, Università Genova, Genova, ITALY

**To cite this Article** Costa, G. , Minicucci, A. , Trefiletti, V. and Valenti, B.(1990) 'Thermotropic liquid-crystalline systems containing methylated rings', *Liquid Crystals*, 7: 5, 629 – 642

**To link to this Article:** DOI: 10.1080/02678299008036747

**URL:** <http://dx.doi.org/10.1080/02678299008036747>

PLEASE SCROLL DOWN FOR ARTICLE

Full terms and conditions of use: <http://www.informaworld.com/terms-and-conditions-of-access.pdf>

This article may be used for research, teaching and private study purposes. Any substantial or systematic reproduction, re-distribution, re-selling, loan or sub-licensing, systematic supply or distribution in any form to anyone is expressly forbidden.

The publisher does not give any warranty express or implied or make any representation that the contents will be complete or accurate or up to date. The accuracy of any instructions, formulae and drug doses should be independently verified with primary sources. The publisher shall not be liable for any loss, actions, claims, proceedings, demand or costs or damages whatsoever or howsoever caused arising directly or indirectly in connection with or arising out of the use of this material.

## Thermotropic liquid-crystalline systems containing methylated rings

by G. COSTA†, A. MINICUCCI‡, V. TREFILETTI† and B. VALENTI‡

† Centro di Studi Chimico-Fisici di Macromolecole Sintetiche e Naturali, CNR,  
Corso Europa 30, 16132 Genova, Italy

‡ Istituto di Chimica Industriale, Università Genova, Corso Europa 30,  
16132 Genova, Italy

(Received 9 August 1989; accepted 6 January 1990)

The thermal properties of low molecular mass and polymeric liquid crystals of similar chemical structure have been investigated in order to see if a parallel structure-properties relationship exists between the two groups of compounds. Two series of models and of the corresponding polymers were prepared, bearing the same mesogenic moiety obtained by reacting 4-hydroxybenzoic acid with different methylated hydroquinones. Ether or ester linkages have been used to bridge the rigid core to the flexible polymethylene spacer. The thermal stability and the nature of the mesophases were examined by different techniques. An interpretation of the results on the basis of the axial ratio and the strength of the orientation-dependent attractions, is attempted for the model compounds. As far as polymers are concerned thermodynamic parameters follow the expected trend if compared with those of low molecular mass analogues. The dependence of the liquid crystal to isotropic transition temperature on the degree of substitution shows the same trend as for the model compounds. Geometric and electronic effects must be taken into account to understand the experimental results.

### 1. Introduction

In order to synthesize polymers with liquid-crystalline properties suitable mesogenic monomers must be used. Convenient melting temperatures can be attained by introducing, between the mesogenic monomers, flexible spacers which increase the entropy of the melt. Moreover the probability of finding a sequence of crystallizable units can be reduced by using asymmetrical moieties with lateral substituents. From the structure-properties relationship of low molecular mass liquid crystals [1] it is known that substituents on the mesogenic unit can reduce the thermal stability of a nematic phase. In fact they can act on the axial ratio of the mesogen, can make the ordering of neighbouring groups more difficult forcing the molecules apart, can cause a steric effect that results in a twisting of the molecular structure and in a reduction of the coplanarity of adjacent groups. However, an increase in the dipolar interactions between neighbouring substituents or substitution in a protected position generally enhances the liquid crystal properties of a mesogen.

The variations, which occur in the thermal stability of the mesophases of semi-rigid thermotropic main-chain polymers as a function of the structure of the mesogenic moieties, have been considered in the recent literature for the role played by three types of modifications. These are (i) changes in the chemical nature of the mesogenic group, (ii) variation of the axial ratio of the rigid core and (iii) the presence of lateral substituents on the aromatic rings [2-5]. It has generally been found that even a slight change in the chemical structure of the mesogenic group can result in a

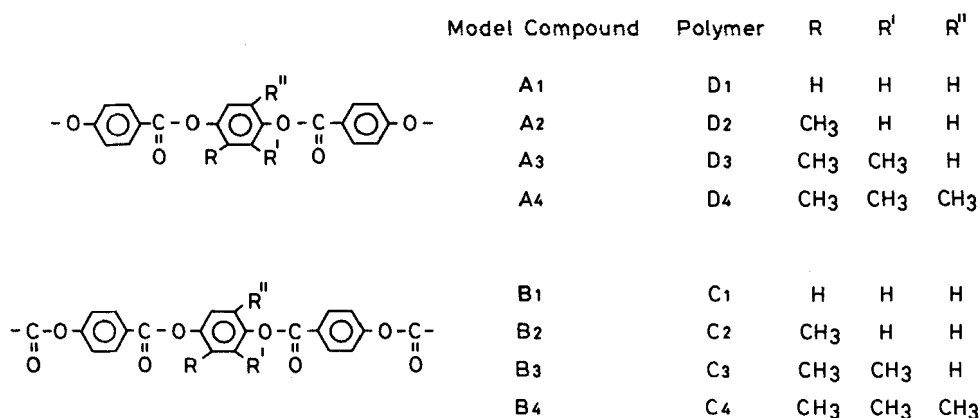


Figure 1. Chemical structures of the mesogenic moieties of model compounds and polymers.

significant variation in the thermal properties of the mesophase [6, 7]. Extensive property modifications seem to occur when substituents are introduced into the mesogenic units [8]. However few systematic studies have been carried out on this topic, particularly on the introduction of several substituents on a mesogenic group. Monosubstitution decreases the liquid crystal–isotropic temperature  $T_i$ , but not necessarily the thermal stability of the mesophase, since the melting point  $T_m$  is, in some cases, more affected than  $T_i$  [9]. The degree of reduction of  $T_i$  is not directly determined by the substituent size only; polar effects can also play an important role [10].

In this paper we report the results obtained for two series of model compounds and polymers, bearing differently methylated central hydroquinone residues. Their chemical structures and reference marks are shown in figure 1. Model compounds A and B have *n*-butyl end groups, whereas polymers D and C have flexible spacers of 12 and 8 methylene units, respectively.

## 2. Experimental

### 2.1. Synthesis of models and polymers

#### 2.1.1. Models A

4-*n*-Butoxybenzoylchloride was prepared by refluxing the corresponding acid, recrystallized from ethanol, with thionyl chloride. Unsubstituted and methylated hydroquinones were recrystallized from toluene. Models A1 and A2 were prepared by dissolving the acid chloride (10 mmol) and the appropriate hydroquinone (5 mmol) in 1,1,2,2-tetrachloroethane (TCE) (overall amount 20 ml) using 10 mmol of freshly distilled triethylamine (Et<sub>3</sub>N) as an acid acceptor [11]. After stirring for 24 hours at room temperature, the final products were precipitated in ethanol and recrystallized in ethylacetate. Yields, 75–90 per cent.

Models A3 and A4 were obtained, following the procedure of Dewar and Schroeder [12], in dry pyridine used as solvent and hydrogen chloride acceptor. For model A3 9 mmol of 4-*n*-butoxybenzoylchloride in 15 ml of pyridine (Py) were added dropwise to a solution of 2,3-dimethylhydroquinone (3 mmol in 15 ml Py). Model A4 was prepared as described previously, by reacting 5 mmol of the acid chloride and 2.5 mmol of diphenol in 7 ml of pyridine. The reaction mixtures were maintained under a nitrogen atmosphere and stirred for 24 hours at room temperature. After adding

dilute hydrochloric acid, the recovered solids were washed with water and stirred for 30 min in 300 ml of 5 per cent aqueous  $\text{NaHCO}_3$ . The resulting compounds were finally filtered, washed with water and recrystallized in ethylacetate and methanol. Yields, 80–90 per cent.

### 2.1.2. Models B

4-Valeryloxybenzoylchloride was synthesized as previously described [11]. Models B1 and B2 were prepared in TCE, using  $\text{Et}_3\text{N}$  as a tertiary amine [11], and recrystallized from ethylacetate and ethanol. Yields, 65–75 per cent.

Model B3 was obtained in dry Py (20 ml) by adding to a solution of the appropriate biphenol (2.7 mmol) the acid chloride (8 mmol). Model B4 was prepared as described for model A4. After stirring for 24 hours at room temperature, the products were isolated from Py as reported before and recrystallized in ethanol and ethylacetate. Yields, 60–70 per cent.

### 2.1.3. Polymers D

4,4'-Dicarboxy- $\alpha,\omega$ -diphenoxydodecane was prepared according to the method described by Griffin and Havens [2] and later on modified by Ober and Bluhm [4]. Ethyl-4-hydroxybenzoate (72.8 mmol) was dissolved in 92 ml of *N,N*-dimethylformamide (DMF). After adding anhydrous sodium carbonate (9.66 g) and 1,12-dibromododecane (36.4 mmol) the reaction mixture was stirred at 150°C for 4 hours. The resulting slurry was cooled, filtered and the solid residue was stirred in 1 l of cold water, filtered and recrystallized in ethanol (yield, 50 per cent; melting point 86°C; elemental analysis: calculated C 72.26 per cent, H 8.49 per cent, found C 72.47 per cent, H 8.53 per cent). The diester 4,4'-dicarbethoxy- $\alpha,\omega$ -diphenoxydodecane was added to a 10 per cent (w/v) solution of potassium hydroxide in 95 per cent ethanol. After stirring under reflux for 5 hours the suspension was diluted with water and acidified with concentrated HCl. The collected solid was washed with water and recrystallized in 2-methoxyethanol (yield, 80 per cent, melting point, 247°C).

4,4'-Dichloroformyl- $\alpha,\omega$ -diphenoxydodecane, obtained by refluxing 4,4'-dicarboxy- $\alpha,\omega$ -diphenoxydodecane with thionyl chloride (melting point 67°C) was dissolved in dry TCE and added dropwise under a nitrogen atmosphere to a stirred solution of an equimolar portion of the appropriate hydroquinone in TCE/ $\text{Et}_3\text{N}$  [11] or Py [2].

Polymerizations D1–D3 were carried out at room temperature or at 50°C for 24–48 hours. Polymer D4 was obtained following the method described by Osman [13]. A solution of the dichloride (8 mmol) in 10 ml of dry TCE was added to a cooled solution of the diphenol (8 mmol) in 6 ml of TCE and 3.2 ml of dry pyridine. After 30 min the temperature was left to rise to room temperature and kept under these conditions for 30 min. The reaction mixture was then heated at 72°C for 2 hours and finally diluted with TCE to 7 per cent concentration (w/v).

All of the polymers were precipitated with methanol, filtered, washed well with water and methanol and dried *i.v.* Polymerization conditions are summarized in table 1.

### 2.1.4. Polymers C

4,4'-(Sebacoyldioxy) dibenzoyldichloride, obtained as previously reported [11] following the procedure of Bilibin *et al.* [14], was dissolved in dry TCE; to this

Table 1. Polymerization conditions (polymers D and C).

Polymer	Et <sub>3</sub> N/dichloride (molar ratio)	Py/dichloride (molar ratio)	Monomer conc. (mol <sup>-1</sup> TCE)	T/°C	t/hour
D1	—	5.0	0.25	50	24
D2 <sup>1</sup>	6.7	—	0.08	Room	48
D2 <sup>2</sup>	—	5.0	0.23	50	24
D3 <sup>1</sup>	—	5.0	0.16	Room	48
D3 <sup>2</sup>	—	5.0	0.21	50	24
D3 <sup>3</sup>	—	7.5	0.26	50	24
D4	—	5.0	1.02	0–72	3
C1	4.7	—	0.11	Room	48
C3 <sup>1</sup>	—	60.0	0.21	Room	48
C3 <sup>2</sup>	—	11.9	0.21	Room	48
C3 <sup>3</sup>	—	11.9	0.21	Room	48
C3 <sup>4</sup>	—	7.8	0.21	Room	48
C3 <sup>5</sup>	2.1	5.9	0.21	Room	48
C4	—	5.0	1.02	0–72	3

solution an equimolar amount of the diphenol in TCE containing Et<sub>3</sub>N or in pyridine was added. After stirring under a nitrogen atmosphere for 48 hours at room temperature (samples C1–C3) or according to [13] (sample C4), the polymers were precipitated in acetone and carefully washed to remove the tertiary amine hydrochloride. The products were finally dried under vacuum. Experimental details are reported in table 1.

### 2.2. Characterization

Conventional tests of structural identification were performed on the reaction intermediates and on the model compounds: elemental analysis and IR spectroscopy (Perkin–Elmer 983). Intrinsic viscosities of the polymeric samples were determined at 25°C in TCE or TCE/phenol 40 : 60 (v/v). Microscopic observations were carried out with a Polyvar Pol Reichert polarizing microscope, equipped with a Mettler FP 82 hot stage (control unit FP 80). Transition temperatures and enthalpies were determined from DSC thermograms recorded with a Mettler TA 3000 system (measuring cell DSC 30) with sample weights from 3 to 9 mg. Heating and cooling rates of 10 K/min were generally used. Thermal profiles were recorded on an Epson mod. PCAX 2 disc memory device and standard data analysis programs were used to evaluate enthalpies and transition temperatures. The thermal stability of the polymeric samples was evaluated by using a Perkin–Elmer TGS 2 analyser, with heating rates of 10 K/min.

### 3. Results and discussion

The series of compounds investigated contain mesogenic moieties built up of three aromatic rings, joined together by ester bridges and connected to flexible end groups or to polymethylene spacers by ether (models A and polymers D) or ester (models B and polymers C) linkages. Our aim in this work was to investigate the thermal properties of stable low molecular mass and polymeric liquid-crystalline materials of similar chemical structure, in order to see if parallel structure–properties relationships exist between the two series of compounds.

Table 2. Elemental analysis of model compounds.

Sample	Percentage C		Percentage H	
	Calculated	Found	Calculated	Found
A1	72.74	72.54	6.49	6.58
A2	73.12	73.34	6.72	6.82
A3	73.49	73.67	6.93	7.03
A4	73.83	73.62	7.14	7.24
B1	69.52	69.29	5.79	5.80
B2 [11]	69.94	69.80	6.01	6.02
B3	70.34	70.62	6.22	6.28
B4	70.73	70.63	6.42	6.42

Table 3. Thermodynamic properties of model compounds.

Model	$T_m/^\circ\text{C}$	$T_{\text{NI}}/^\circ\text{C}$	$\Delta H_m/\text{kJ mol}^{-1}$	$\Delta H_{\text{NI}}/\text{kJ mol}^{-1}$	$\Delta S_{\text{NI}}/\text{J mol}^{-1} \text{K}^{-1}$
A1	154.1	244.2	34.3	2.85	5.52
A2	112.5	202.8	33.5	2.93	6.15
A3	136.8	226.6	30.5	3.51	7.03
A4	139.2	188.9	30.1	3.56	7.70
B1	166.5	261.5	28.5	1.88	3.51
B2†	125.1	215.7	41.4	1.80	3.68
B3	118.8	248.1	27.2	2.38	4.56
B4	115.1	207.2	25.9	2.18	4.52

† From [11].

We consider first the liquid crystal behaviour of monomeric models. Their elemental analysis characterizations are reported in table 2; IR spectra appear to be consistent with the required chemical structures. The results of the DSC investigations are listed in table 3. All of the esters synthesized exhibit a nematic phase with large stability range; transition temperatures have been checked both by DSC and optical observations. Models A1 and A2 have been reported previously [4, 5, 12, 15–18]; melting points of 153–158°C and 115.3°C, liquid crystal–isotropic transition temperatures of 241–245°C and 206°C were indicated for A1 and A2, respectively. Transition enthalpies consistent with our results have been also obtained [4, 5]. Included in the same table are the thermodynamic properties of model B2, which we have recently considered [11].

The data in table 3 indicate that, as one methyl group is appended to the central hydroquinone residue of the mesogenic models, the stability range of the nematic phase is shifted towards lower values. The melting point is depressed and the nematic–isotropic transition temperature  $T_{\text{NI}}$  decreases for both series, with ranges between 40 and 50°C. However, the introduction of a 2,3-dimethylhydroquinone group enhances the liquid crystal properties of models A3 and B3, which show higher  $T_{\text{NI}}$  than the corresponding monosubstituted compounds A2 and B2. Further introduction of a  $\text{CH}_3$  group on the 5-position of the hydroquinone ring results, as expected, in a reduction of the nematic range. Comparable values of nematic–isotropic transitional enthalpy and entropy are found for unsubstituted and mono-methylated models; for disubstitution the enhanced mesophase stability is coupled with higher values of  $\Delta H_{\text{NI}}$  and  $\Delta S_{\text{NI}}$ . No appreciable variation appears on going from disubstituted to tri-substituted compounds. By comparing series A and B with each other, we can observe that models B show higher  $T_{\text{NI}}$  but lower  $\Delta H_{\text{NI}}$  and  $\Delta S_{\text{NI}}$ .

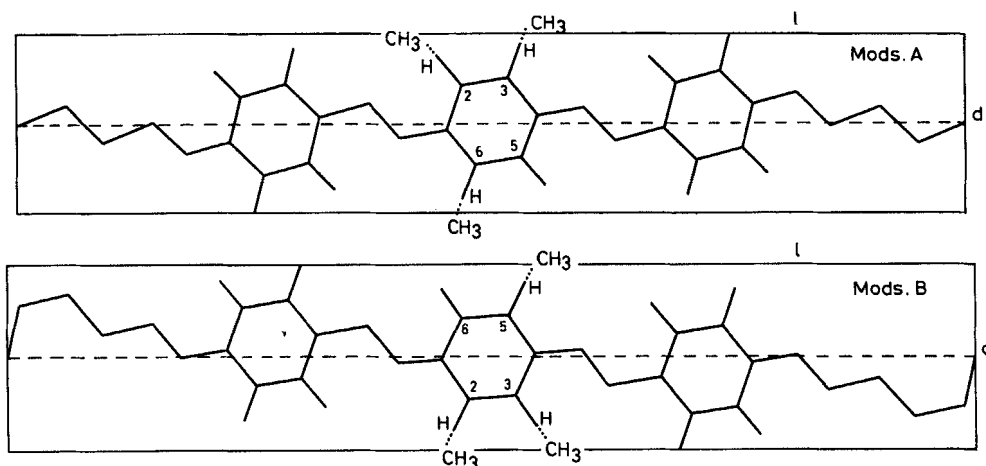


Figure 2. The molecular structures of models A and B (model A1  $l = 31.46 \text{ \AA}$ ,  $d = 7.74 \text{ \AA}$ ,  $x = 4.06$ ; model B1  $l = 31.66 \text{ \AA}$ ,  $d = 8.28 \text{ \AA}$ ,  $x = 3.82$ ).

In order to understand better the effect of lateral substitution on mesophase stability, we have tried to interpret our results in terms of the variation of the two parameters introduced by Flory and Ronca [19] to relate the characteristics of the nematic–isotropic transition to the molecular structure. They are the length-to-diameter axial ratio  $x (\equiv l/d)$  of the molecule, assumed to be cylindrically symmetric about the long axis, and the characteristic temperature  $T^*$ , which measures the strength of the orientation dependent mutual attractions between molecules. Experimental transition temperatures for rod-like nematics can be compared with theory on the basis of

$$\bar{T}_{NI} = T_{NI}/xT^*, \quad (1)$$

which relates the transition temperature  $T_{NI}$  to the parameters  $x$  and  $T^*$ , through the reduced temperature  $\bar{T}_{NI}$ .

As evidenced in figure 2, the molecular structure of models A and B shows significant departures from cylindrical symmetry. The *p*-phenylene residues define three axes that are approximately parallel but not collinear. Coplanarity of the ester and phenylene groups can be assumed; however steric interactions in methylated models could introduce departures from coplanarity. Significant rotations around several of the skeletal bonds could allow a variety of conformations. Additional departures of these molecules from cylindrical symmetry could result from articulations of the terminal *n*-butyl groups. However, as suggested by Flory and Ronca for a few typical nematics [19], mutual alignment of the molecules in the nematic phase may require adoption of a certain uniformity in conformation, unlike the isotropic state. On this basis, even if our representation of models A and B shown in figure 2 is idealized, we believe that qualitatively it can be used, since we are comparing molecules with the same basic chemical structure.

Consequently we have assumed models A1 and B1 to be represented by two cylinders, whose maxima longitudinal sections are indicated in figure 2. The axial ratios of the molecules are calculated from the dimensions  $l$  and  $d$  of the cylinder sections, obtained from bond lengths and angles (data from [20]) assuming van der Waals' radii of 1.2 and 2.0  $\text{\AA}$  for H and  $\text{CH}_3$ , respectively. Moreover the conformations

Table 4. Nematic-isotropic transitions and axial ratios of model compounds

Model	<i>R</i>	<i>R'</i>	<i>R''</i>	<i>T</i> <sub>Ni</sub> /K	<i>l</i> /Å	<i>d</i> /Å	<i>x</i>
A1	H	H	H	517.2	31.46	7.74	4.06
A2	CH <sub>3</sub>	H	H	475.8	31.46	<8.64>	<3.64>
A3	CH <sub>3</sub>	CH <sub>3</sub>	H	499.6	31.46	8.85	3.55
A4	CH <sub>3</sub>	CH <sub>3</sub>	CH <sub>3</sub>	461.9	31.46	<9.75>	<3.23>
A5	C <sub>2</sub> H <sub>5</sub>	H	H	431.0†	31.46	<9.26>	<3.40>
A6	C <sub>3</sub> H <sub>7</sub>	H	H	399.0†	31.46	<9.86>	<3.19>
A7	C <sub>4</sub> H <sub>9</sub>	H	H	383.0†	31.46	<10.28>	<3.06>
A8	C <sub>11</sub> H <sub>23</sub>	H	H	(344.0)†	31.46	<10.44>	<3.01>
B1	H	H	H	534.5	31.66	8.28	3.82
B2	CH <sub>3</sub>	H	H	488.7	31.66	<8.81>	<3.59>
B3	CH <sub>3</sub>	CH <sub>3</sub>	H	521.1	31.66	8.90	3.56
B4	CH <sub>3</sub>	CH <sub>3</sub>	CH <sub>3</sub>	480.2	31.66	<9.43>	<3.36>

† Data from [5, 18]. Model A8 is reported to exhibit a monotropic transition to a nematic state.

of the terminal *n*-butyl chains which approach most closely a cylindrical compact rod-like shape have been considered (all trans for models A and trans, apart from the terminal C–C bond, for models B).

Lateral substitution acts to increase the cylinder diameters; the mean values *d* of models A2, B2 and A4, B4 have been calculated by averaging the results estimated by considering substitution on the 2 or 3 and 5 or 6 positions of the hydroquinone ring. Only one possibility must be considered for models A3 and B3. The estimated mean axial ratios are given in table 4, together with the nematic-isotropic transition temperatures. We have added to our results some literature data [5, 18] on the transition temperatures for compounds of the A series having one *n*-alkyl substituent (from C<sub>2</sub>H<sub>5</sub> to C<sub>11</sub>H<sub>23</sub>) on the hydroquinone residue. Bond rotations in the *n*-alkyl chains of compounds A5–A8 permit a range of conformations, which significantly affect the form of the molecules; some of them are effectively precluded by steric interactions with the phenylene ring. We have estimated the diameters of all conformers for compounds A5, A6 and A7, considering substitution on the 2 and 3 position of the ring. The variation of both *d* and *x* are listed in table 5; the mean values of the diameters and the axial ratios are reported in table 4. For model A8, having a C<sub>11</sub>H<sub>23</sub> substituent, the mean diameter has been calculated assuming, to a first approximation,

Table 5. Variation ranges of diameters and axial ratios.

Model	Diameter range/Å	Axial ratio range
A1	7.74	4.06
A2	8.43–8.85	3.55–3.73
A3	8.85	3.55
A4	9.54–9.96	3.16–3.30
A5	8.43–9.93	3.17–3.73
A6	8.43–11.36	2.77–3.73
A7	8.43–12.44	2.53–3.73
A8	10.34–10.54	2.98–3.04
B1	8.28	3.82
B2	8.72–8.90	3.56–3.63
B3	8.90	3.56
B4	9.34–9.52	3.33–3.39



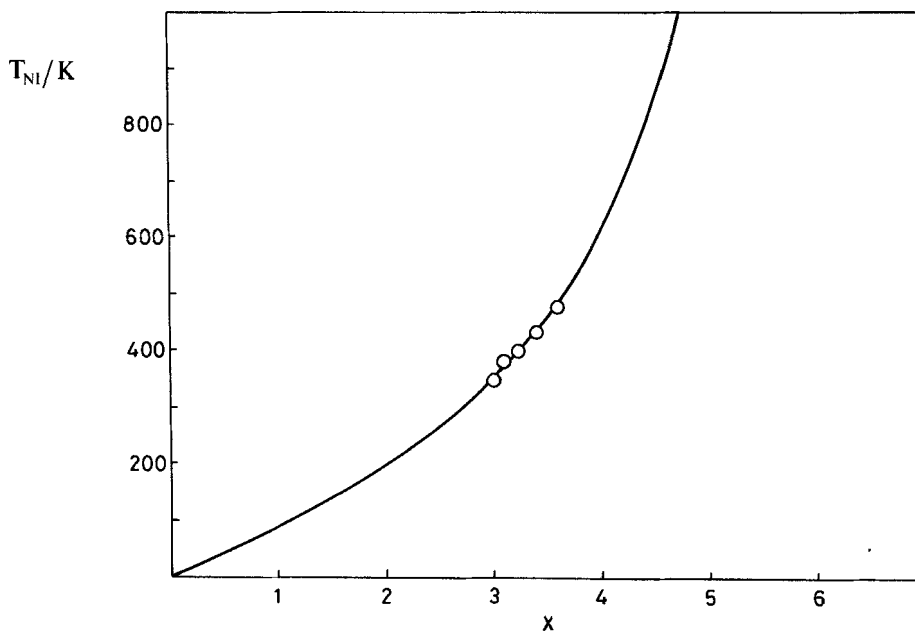


Figure 3.  $T_{\text{NI}}$  values as a function of the axial ratio for monosubstituted models A. The calculated curve refers to  $T^*$  of 337 K.

that the spatial extension of the flexible appendage might be expressed by the end-to-end distance of the  $\text{C}_{11}\text{H}_{23}$  group, i.e. the root-mean-square average of the separation between the two ends of the alkyl chain (given by  $nl^2$ , where  $n$  is the number of bonds and  $l$  the C–C bond length).

Values of  $T^*$  deduced from axial ratios and the  $T_{\text{NI}}$  range between 320 and 350 K for monosubstituted models of series A.  $T_{\text{NI}}$  data are plotted in figure 3 against the axial ratio; the theoretical curve is derived from [19] assuming  $T^*$  to be 337 K. The main result is that monosubstituted A compounds exhibit similar  $T^*$  and therefore comparable orientation-dependent interactions. However lower  $T^*$  values would have been expected, in view of the low anisotropy of polarizability of the terminal  $-\text{OC}_4\text{H}_9$  groups and of the values of  $T^*$  reported for conventional nematics in [19]. As discussed by Flory and Ronca, for molecules such as *p*-azoxyanisole or *p*-azoxyphenetole, the displacement of the phenyl axes from collinearity can introduce a plate-like shape to some extent. Consequently  $T^*$  values might be over-estimated, because of the greater asymmetry of the molecules, underestimated by the axial ratio.

Other effects, such as departure from coplanarity, due to steric interactions in the substituted models or the variety of conformations of the terminal chains can be neglected, since they should result in an overestimate of the axial ratio and consequently in an underestimate of  $T^*$ .

$T^*$  values calculated for models A1–A4 and B1–B4 are reported in table 6. What appears is that, for both series,  $T^*$  increases with the degree of substitution. The strength of the orientation-dependent mutual attractions between molecules is enhanced by the presence of  $\text{CH}_3$  groups on the ring, which alter the electronic distribution in the resulting compounds, favouring molecular packing in the nematic state (the latent enthalpy for the transition increases with substitution, see table 3). Models B exhibit higher  $T^*$  than As for low degrees of substitution, comparable

Table 6. Estimate of the characteristic temperature  $T^*$  for models A and B.

Model	$T^*/\text{K}$
A1	274
A2	321
A3	354
A4	390
B1	325
B2	339
B3	367
B4	378

Table 7. Yields and intrinsic viscosities of polymers D and C.

Polymer	Yield/per cent	$[\eta]/\text{dl g}^{-1}$
D1	89	0.30†
D2 <sup>1</sup>	74	0.15‡
D2 <sup>2</sup>	87	0.39†
D3 <sup>1</sup>	54	0.10‡
D3 <sup>2</sup>	70	0.49†
D3 <sup>3</sup>	90	0.78†
D4	72	0.20‡
C1	75	0.30†
C2 <sup>1</sup> §	85	0.53‡
C2 <sup>2</sup> §	81	0.70‡
C3 <sup>1</sup>	44	0.23‡
C3 <sup>2</sup>	51	0.31‡
C3 <sup>3</sup>	80	0.21‡
C3 <sup>4</sup>	90	0.21‡
C3 <sup>5</sup>	50	0.23‡
C4	94	0.40‡

† Measured in TCE/phenol 40 : 60 (v/v) at 25°C.

‡ Measured in TCE at 25°C.

§ Data from [11, 21].

values have been derived for di and trimethylated models. Intermolecular interactions, due to the external ester groups, might play a role for B1 and B2 models, until the asymmetry of the electronic distribution on the central ring becomes the prevailing factor. The transition enthalpies and entropies are lower for B than for A models; association of the molecules in the isotropic state, due to the polar  $-\text{COO}-$  groups in the tails, might provide an explanation for this result.

Yields and intrinsic viscosities of polymers D and C are listed in table 7. As extensively described elsewhere for polymer C2 [21], the type and amount of tertiary amine, monomer concentration and reaction conditions strongly affect the polymer characteristics. The thermal behaviour was investigated by both DSC and optical microscopy. The thermodynamic properties are collected in table 8. The molecular mass which affects the values of the transition temperatures and the polydispersity of chain lengths gives rise to broad isotropization endotherms (as apparent in figure 4).

Polymers D1 and D3 exhibit nematic and smectic mesophases. The DSC profile reveals three endotherms on heating and two exotherms on cooling from the isotropic state, which correspond, from optical observations, to the appearance of the nematic

Table 8. Thermodynamic properties of the polyesters

Polymer	$T_{CC}/^{\circ}\text{C}$	$T_m/^{\circ}\text{C}$	$T_{SN}/^{\circ}\text{C}$	$T_{NI}/^{\circ}\text{C}$	$\Delta H_m/\text{kJ mol}^{-1}$	$\Delta H_{SN}/\text{kJ mol}^{-1}$	$\Delta H_{NI}/\text{kJ mol}^{-1}$	$\Delta S_{NI}/\text{J mol}^{-1}\text{K}^{-1}$
D1	—	129.2	228.5	279.1	5.0	4.6	6.3	11.7
D2	—	164.1	—	226.7	10.5	—	7.1	14.2
D3 <sup>2</sup>	—	146.5	205.8	256.9	10.0	10.0	5.0	9.6
D3 <sup>3</sup>	—	145.7	213.3	269.5	7.5	11.7	7.5	13.8
D4	—	198.8	—	212.0	9.2	—	5.4	11.3
C1	—	231.0	—	$T_D^\dagger$	2.9	—	—	—
C2 <sup>1†</sup>	—	188.6	—	304.4	4.2	—	9.6	16.7
C2 <sup>2†</sup>	102.0	206.7	—	323.1	9.6	—	8.4	14.2
C3 <sup>4</sup>	106.0	198.0	—	330.0	10.9	—	7.1	11.7
C4	—	244.9	—	313.6	6.3	—	6.7	11.7

† Data from [11, 21].

‡  $T_D$  decomposition temperature.

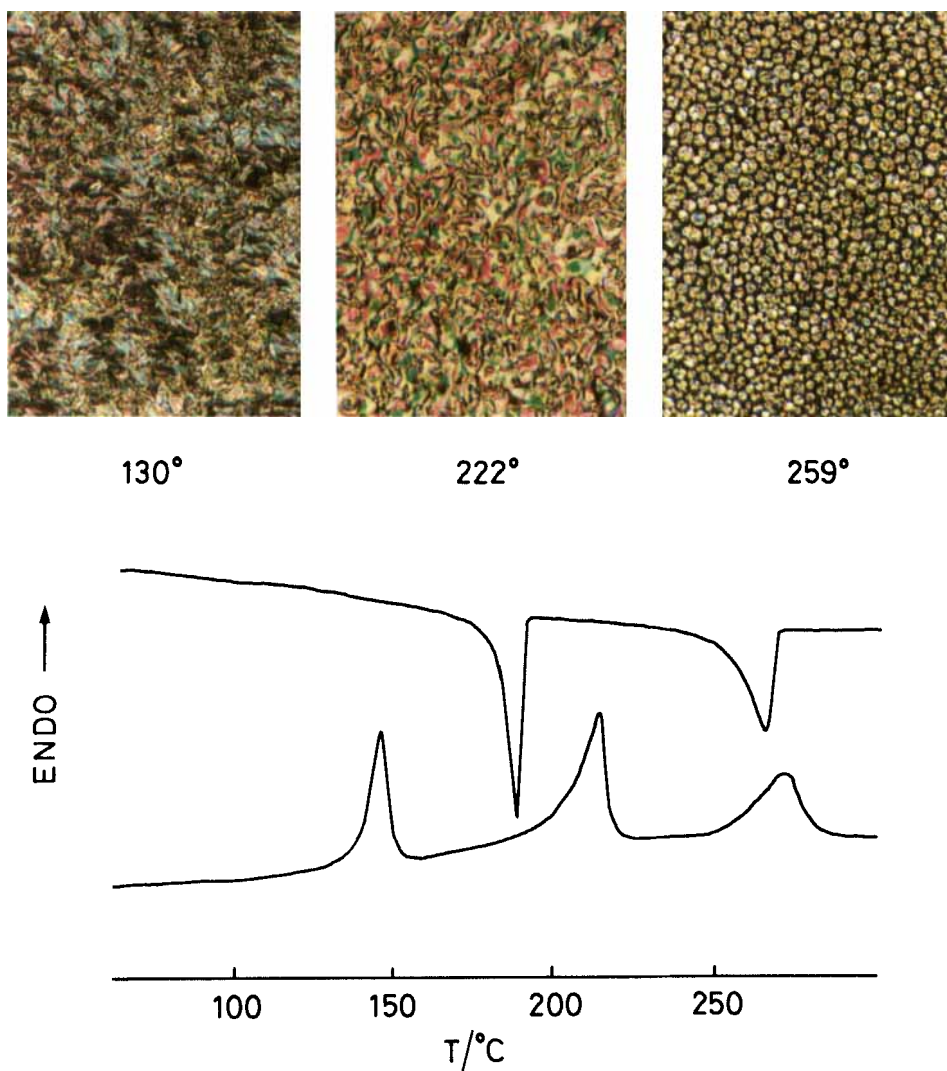


Figure 4. The DSC profiles obtained at  $10 \text{ K min}^{-1}$  and the optical textures (259, 222 and  $130^\circ\text{C}$  on cooling from the isotropic state) of polymer D3.

state and to the transition to a smectic A or C phase (see figure 4). The lower temperature mesophase is frozen in the glassy polymers. Polymer D1 was also reported by Ober and Bluhm to exhibit a smectic and a nematic phase; transition temperatures of 137, 221 and  $271^\circ\text{C}$  have been found for a sample of limiting viscosity number  $0.2 \text{ dl g}^{-1}$  [4].

Polymer D2 and D4, probably because of the asymmetry of their mesogenic moieties, appear to be only nematogenic (two peaks in the DSC heating profile and one on cooling; see figure 5). The nematic–isotropic transitions are almost reversible, whereas a supercooling of about  $20^\circ\text{C}$  is observed at the nematic–smectic transition. As for models A, the introduction of a second  $\text{CH}_3$  group on the hydroquinone ring enhances the thermal stability of the mesophase; further substitution has a destabilizing effect.

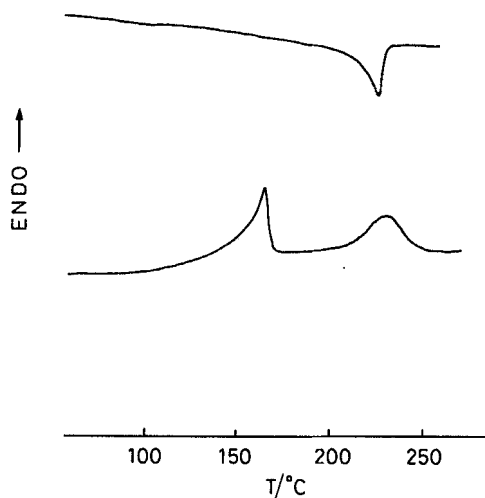


Figure 5. The heating and cooling curves obtained at  $10 \text{ K min}^{-1}$  for polymer D2.

Polymers C are only nematogenic. As polymerized C2 and C3 samples exhibit, on heating, a low temperature solid–solid transitions, evidenced by DSC and X-ray analysis and discussed in detail in [21]. Whereas polymer C2 seems to have a hexagonal packing with an interchain distance of  $5.1 \text{ \AA}$  and a longitudinal spacing of  $16.3 \text{ \AA}$ , polymer C3 diffraction patterns reveal, at wide angles, two sharp reflections, which should be characteristic of a rectangular array, and at small angles a spacing of  $20.5 \pm 0.2 \text{ \AA}$ . In both polymers, after a heating cycle, this low temperature transition disappears and only melting and formation of the isotropic phase can be observed.

The nematic–isotropic temperature of polymer C1 cannot be determined, since decomposition starts at lower temperature; substituted polyesters show clearing points higher than  $300^\circ\text{C}$ . C2 samples show the molecular mass dependence of the transition temperatures; for C3 with  $[\eta] = 0.21 \text{ dl g}^{-1}$ ,  $T_{\text{NI}}$  is close to  $330^\circ\text{C}$ , with a very broad transition peak. Again disubstitution enhances this transition. Sample C4, in spite of the large degree of substitution, is nematic over a  $60^\circ\text{C}$  range and has a high nematic–isotropic transition temperature. For this series of polyesters crystallization can be observed, beyond a certain value of the molecular mass, only if the heating cycle is stopped in the nematic range, just below the  $T_{\text{NI}}$ .

As expected the nematic–isotropic transitional enthalpies and entropies are substantially larger than those determined for the model compounds; in contrast the enthalpy changes on polymer melting are considerably lower than those of models A and B. These results, which reflect the lack of ability of polymers to form crystal structures of high packing order, suggest on the other hand, that in the polymer the flexible chains participate in the ordered liquid crystal regions [2, 22–24].

We can conclude that, qualitatively, the models and the polymers with the same chemical structure exhibit parallel structure–properties relationships. Although for polymers it is more difficult to find theoretical support for the interpretation of the experimental results, it is interesting to observe in figure 6 the analogous behaviour of low and high molecular mass systems, as a function of the degree of substitution.

The difference in nematic–isotropic transition temperatures existing between polymers C and D arises only partially from the different chemical structure of the

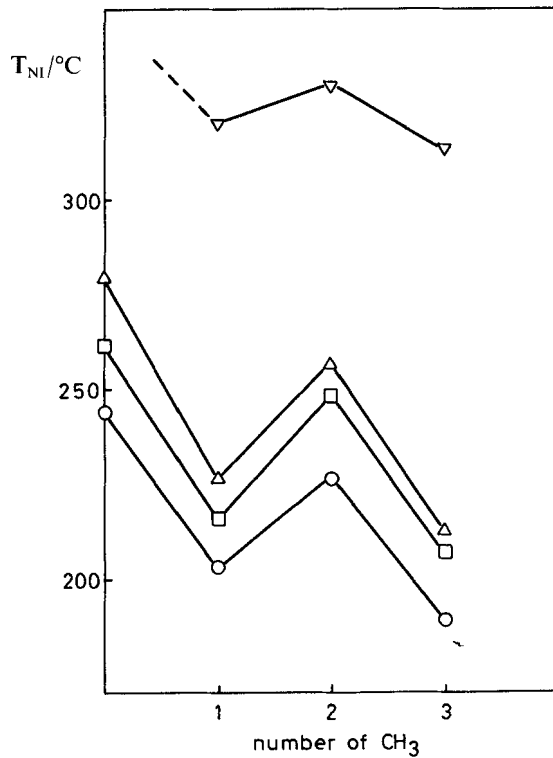


Figure 6. The nematic-isotropic transition temperatures as a function of the degree of substitution for models A (O) and B (□) and polymers C (▽) and D (△).

two series of compounds. The main factor is the variation in the length of the flexible polymethylene chain of the repeating unit.

The authors thank Dr. B. Gallot (CNRS, Vernaison, France) for performing X-ray experiments and Dr. E. Marsano for a useful discussion. Partial support of this work from the Ministero Pubblica Istruzione is acknowledged.

#### References

- [1] GRAY, G. W., 1982, *Polymer Liquid Crystals*, edited by A. Ciferri, W. R. Krigbaum and R. B. Meyer (Academic Press), p. 1.
- [2] GRIFFIN, A. C., and HAVENS, S. J., 1981, *J. Polym. Sci. Polym. Phys. Ed.*, **19**, 951.
- [3] BLUMSTEIN, A., 1985, *Polym. J.*, **17**, 277.
- [4] OBER, C. K., and BLUHM, T. L., 1986, *Polym. Bull.*, **15**, 233.
- [5] LENZ, R. W., 1985, *Pure appl. Chem.*, **57**, 1537.
- [6] LENZ, R. W., 1985, *Polym. J.*, **17**, 105.
- [7] COSTA, G., NORA, A., TREFILETTI, V., and VALENTI, B., 1988, *Molec. Crystals liq. Crystals*, **157**, 79.
- [8] OBER, C. K., JIN, J.-I., and LENZ, R. W., 1984, *Adv. Polym. Sci.*, **59**, 103.
- [9] ANTOUN, S., LENZ, R. W., and JIN, J.-I., 1981, *J. Polym. Sci. Polym. Chem. Ed.*, **19**, 1901.
- [10] LENZ, R. W., 1985, *J. Polym. Sci. Polym. Symp.*, **72**, 1.
- [11] VALENTI, B., TREFILETTI, V., SILANUS, F., and COSTA, G., 1988, *Molec. Crystals liq. Crystals*, **155**, 511.
- [12] DEWAR, M. J. S., and SCHROEDER, J. P., 1965, *J. org. Chem.*, **30**, 2296.
- [13] OSMAN, M. A., 1986, *Macromolecules*, **19**, 1824.

- [14] BILIBIN, A. YU., TENKOVITSEV, A. V., and SKOROKHODOV, S. S., 1985, *Makromolek. Chem. rap. Commun.*, **6**, 209.
- [15] DEWAR, M. J. S., and GOLDBERG, R. S., 1970, *J. org. Chem.*, **35**, 2711.
- [16] GRIFFIN, A. C., WERTZ, O. L., and GRIFFIN, A. C., JR., 1978, *Molec. Crystals liq. Crystals*, **44**, 267.
- [17] SCHROEDER, J. P., 1980, *Molec. Crystals liq. Crystals*, **61**, 229.
- [18] WEISSFLOG, W., and DEMUS, D., 1984, *Crystal Res. Technol.*, **19**, 55.
- [19] FLORY, P. J., and RONCA, G., 1979, *Molec. Crystals liq. Crystals*, **54**, 311.
- [20] SUTTON, L. E. (editor), 1958, *Tables of Interatomic Distances and Configuration in Molecules and Ions* (The Chemical Society), and 1965, Supplement.
- [21] COSTA, G., TREFILETTI, V., VALENTI, B., and GALLOT, B., 1990, *Makromolek. Chem.*, **191**.
- [22] GREBOWICZ, J., and WUNDERLICH, B., 1983, *J. Polym. Sci. Polym. Phys. Ed.*, **21**, 141.
- [23] BLUMSTEIN, A., and THOMAS, O., 1982, *Macromolecules*, **15**, 1264.
- [24] MARSANO, E., and VALENTI, B., 1989, *Molec. Crystals liq. Crystals* (in the press).